

The NGC 300 Transient: An Alternative Method For Measuring Progenitor Masses

Stephanie M. Gogarten¹, Julianne J. Dalcanton^{1,2}, Jeremiah W. Murphy^{1,3}, Benjamin F. Williams¹, Karoline Gilbert¹, Andrew Dolphin⁴

ABSTRACT

We present an alternative technique for measuring the precursor masses of transient events in stars undergoing late stage stellar evolution. We use the well-established techniques of stellar population modeling to age-date the stars surrounding the site of the recent transient event in NGC 300 (NGC 300 OT 2008-1). The surrounding stars must share a common turn-off mass with the transient, since almost all stars form in stellar clusters that remain physically associated for periods longer than the lifetime of the most massive stars. We find that the precursor of NGC 300 OT 2008-1 is surrounded by stars that formed in a single burst between 8–13 Myr ago, with 70% confidence. The transient was therefore likely to be due to a progenitor whose mass falls between the main sequence turn-off mass (12 M_{\odot}) and the maximum stellar mass (25 M_{\odot}) found for isochrones bounding this age range. We characterize the general applicability of this technique in identifying precursor masses of historic and future transients and supernovae (SNe), noting that it requires neither precursor imaging nor sub-arcsecond accuracy in the position of the transient. It is also based on the well-understood physics of the main sequence, and thus may be a more reliable source of precursor masses than fitting evolutionary tracks to precursor magnitudes. We speculate that if the progenitor mass is close to 17 M_{\odot} , there may be a connection between optical transients such as NGC 300 OT 2008-1 and the missing type II-P SNe, known as the "red supergiant problem."

Subject headings: galaxies: individual (NGC 300) | galaxies: stellar content | stars: evolution

¹Department of Astronomy, University of Washington, Box 351580, Seattle, WA 98195; stephanie@astro.washington.edu

²Wycko Faculty Fellow

³N SF Astronomy and Astrophysics Postdoctoral Fellow

⁴Raytheon; 1151 E. Hemans Rd., Tucson, AZ 85706

1. Introduction

Energetic and luminous transients mark the final stages of massive stars' evolution. These transients include core-collapse explosions leading to Type II and Ib/c supernovae (SNe), luminous blue variable (LBV) outbursts, and other more mysterious transients such as the optical transients in NGC 300 (hereafter NGC 300 OT 2008-1, following Berger et al. 2009) and NGC 6946 (SN 2008S; Prieto et al. 2008a). Current stellar evolution models indicate that the mapping between progenitor stars and the type of supernova is determined primarily by the zero age main-sequence mass and the star's mass-loss history. The theoretical expectations are that the most massive stars ($> 25 M_{\odot}$) experience tremendous mass loss at the end of their lives, expelling their hydrogen and/or helium envelopes before exploding as SN Type Ib/c; somewhat less massive stars ($10\text{--}25 M_{\odot}$) are assumed to lose less mass as they evolve, and explode as SN Type II with their hydrogen envelopes intact (Woosley et al. 2002; Heger et al. 2003; Limongi & Chieffi 2007). This picture is supported by observations (James & Anderson 2006; Prieto et al. 2008b; Kelly et al. 2008; Anderson & James 2008). On the other hand, theoretical expectations for the progenitors of optical transients such as NGC 300 OT 2008-1 and SN 2008S are lacking. Empirically, LBVs are expected to be $\sim 20 M_{\odot}$ (Smith et al. 2004; Smith 2007) and estimates for NGC 300 OT 2008-1 and SN 2008S place the progenitor mass somewhere between 6 and $20 M_{\odot}$ (Prieto et al. 2008a; Thompson et al. 2008; Smith et al. 2009; Bond et al. 2009; Botticella et al. 2009). However, it is unclear whether the latter are SNe resulting from the collapse of O/Ne cores (hereafter referred to as "electron-capture SNe"; Prieto et al. 2008a; Thompson et al. 2008; Botticella et al. 2009), an extension of the LBV outburst phenomena to lower masses (Smith et al. 2009), or a new class of transient due to an unknown mechanism.

At this juncture, progress in understanding the origins of these transients would be aided by the addition of observational constraints. The increasing prevalence of time-domain observations is adding to the number of transients identified, but the most basic property of the transients—their stellar mass—remains largely unknown.

One approach to constraining the masses of the stars showing transients is to use precursor imaging (e.g., Smartt et al. 2009). If images of a star exist before outburst, stellar evolutionary tracks that pass through the color and magnitude of the likely precursor can then be used to estimate the star's initial main-sequence mass. Core-collapse explosions which disrupt the star require precursor imaging to identify the progenitor, whereas imaging after the transient is possible for LBVs and other transients that do not completely disrupt the star. This second class of objects can be misidentified as SNe and has been labeled "SN impostors" (Van Dyk 2007).

Several groups have noted two unusual transients discovered in 2008 with spectra similar to Type II SNe, but whose luminosities are much lower than typical SNe (Stanishev et al. 2008; Bond et al. 2008; Monard 2008; Bond et al. 2009; Berger et al. 2009). These two transients—SN 2008S and NGC 300 OT 2008-1—have no optical precursor, but do show a very red source in the mid-IR bands covered by IRAC and MIPS on the Spitzer Space Telescope (Berger & Soderberg

2008a,b; Prieto 2008; Prieto et al. 2008a; Bond et al. 2009; Berger et al. 2009). These two precursors have been interpreted as defining a new class of heavily dust enshrouded super asymptotic giant branch (AGB) stars, which may have exploded as electron-capture SNe (Prieto et al. 2008a; Thompson et al. 2008; Botticella et al. 2009). Alternatively, Smith et al. (2009) suggest that SN 2008S is not a core-collapse supernova, electron-capture or otherwise. They instead propose that SN 2008S is a "SN impostor" with a super-Eddington wind emanating from a star with mass $\approx 15 M_{\odot}$.

Recent light curve and spectroscopic observations of NGC 300 OT 2008-1 confirm its overall similarity to SN 2008S (Bond et al. 2009; Berger et al. 2009). The spectra show evidence for both a wind and fallback of material from a previous mass-loss event. However, due to the uncertainties in stellar evolution models, translating bolometric luminosities to mass estimates results in a fairly broad range of possible masses for these stars.

While direct imaging of precursors clearly has promise for estimating masses, it suffers from a number of substantial limitations. First among these is the requirement that the precursor actually exists. The majority of past transients have neither pre-existing Hubble Space Telescope (HST) imaging, nor sufficiently accurate astrometry. The second major limitation is that even when precursor imaging is available, interpretation of that imaging depends on the most uncertain stages of stellar evolution (e.g., Gallart et al. 2005). Existing studies typically estimate the mass of a precursor by fitting evolutionary tracks to its color and magnitude. However, uncertainties in stellar evolution models related to rotation, mass loss, pulsation, internal mixing, the formation of dust in stellar winds, and convective instabilities in shell-burning layers all contribute some difficulty in determining the mass of a single highly-evolved star (see discussion in §4.3.5).

In this paper, we demonstrate an alternative approach using stellar populations. Our method is based on the fact that most transient events occur in the last stages of stellar evolution and within groups of stars that share a common age and metallicity. Thus, even after an individual star has evolved, the remaining stars still provide information about the age of the stellar population that hosted the transient, even if the source of the transient is no longer visible. Once that age is known, one can infer the mass of the star that exhibited the transient, since it likely corresponds to a star that has recently turned off the main sequence.

This method has been used to age-date SNe for which the surrounding stars could be resolved. Efremov (1991) identified a young cluster surrounding SN 1987A and estimated its age as ≈ 10 Myr; this estimate was later refined to 12 ± 4 Myr (Walton et al. 1993) and then 12 ± 2 Myr (Panagia et al. 2000). Van Dyk et al. (1999) studied stellar populations in the vicinity of a number of SNe and were able to estimate progenitor masses in a few cases. Maza-Pellániz et al. (2004) and Wang et al. (2005) estimated the age and mass of SN 2004dj using not resolved stars in its originating cluster but by finding the combination of spectral energy distributions (SEDs) which best fit the integrated cluster light. They arrived at age estimates of 13.6 Myr and 20 Myr, respectively, which correspond to progenitor masses of 15 and $12 M_{\odot}$. Vinko et al. (2009) t

isochrones to the color-magnitude diagram (CMD) of resolved stars in this cluster and placed the age at $10\{16$ M yr, corresponding to a progenitor mass of $12\{20$ M_{\odot} . Crockett et al. (2008) attempted to date SN 2007gr using SED fitting, but found two possible solutions at $7\{0.5$ M yr and $20\{30$ M yr.

Our method takes advantage of the fact that most stars form in stellar clusters with a common age ($t_{\text{cl}} \sim 3\{5$ M yr) and metallicity. Indeed, over 90% of stars form in rich clusters containing more than 100 members with $M > 50$ M_{\odot} (Lada & Lada 2003). The stars which formed in a common event remain spatially correlated on physical scales up to ~ 100 pc during the 100 M yr lifetimes of $4 M_{\odot}$ stars, even if the cluster is not gravitationally bound (Bastian & Goodwin 2006); we have confirmed this expectation empirically in Gogarten et al. (2009). Thus, it is reasonable to assume that most young stars within approximately a hundred parsecs of a massive-star transient are coeval. The age of a transient's host stellar population can then be recovered from the CMD of the surrounding stars, using well-established methods for deriving the star formation history (SFH).

Herein, we analyze the specific case of NGC 300 OT 2008-1, by extracting stars from a small aperture around the location of the transient, using photometry from the ACS Nearby Galaxy Survey Treasury (ANGST; Dalcanton et al. 2009). Using the methods described in Williams et al. (2009) and Gogarten et al. (2009), we solve for the SFH in the region of the transient. We find a very well-defined burst of star formation that occurred $8\{13$ M yr ago. The burst allows us to accurately age-date the evolving stellar population which produced the transient. The mass of the transient can then be linked to the masses of stars that have recently turned off the main sequence but have not yet exploded, which in this case is $12\{25$ M_{\odot} . We will show that with this method, it is possible to establish limits on the mass of the precursor, using only imaging taken after the transient itself.

The outline of the paper is as follows. In §2 we discuss the stellar photometry used to analyze the age of the transient. In §3.1 we discuss the recovery of the SFH. In §3.2 we calculate the resulting stellar mass of the main sequence star which evolved to produce the transient. In §4 we discuss the implications of our results, strategies for expanding the use of this method, and possible limitations. We conclude with §5.

2. Data and Photometry

The location of NGC 300 OT 2008-1 ($\alpha = 00^{\text{h}}54^{\text{m}}34.552^{\text{s}}$, $\delta = 37^{\circ}38'31.7900''$ (J2000), Berger & Soderberg 2008b) is contained both in one of our ANGST fields observed 2006 November 8, and in an archival observation taken 2002 December 25. The ANGST data had exposure times of 1488s in F475W, 1515s in F606W, and 1542s in F814W. The archival data had exposure times of 1080s in F435W and F555W, and 1440s in F814W. Each of these observations was split into two exposures, which were calibrated and stacked using the standard HST pipeline. Photometry was done using

DOLPHOT, a modified version of HST phot (Dolphin 2000) optimized for ACS. Details of the photometry and quality cuts used for the ANGST sample and archival data are given in Williams et al. (2009) and Dalcanton et al. (2009). We use only the highest-quality photometry for this analysis. Although the ANGST data was in fact taken before the transient occurred, there is no star visible at the location of the transient (Bond et al. 2009), and thus the precursor was not visible at optical wavelengths.

Artificial stars, used to characterize the completeness of the photometry, were inserted and detected using DOLPHOT. We have approximately 200,000 artificial stars for each field in the region in which both the archival and ANGST fields overlap. We use fake stars only for the overlap region so the effects of crowding will be identical for the two fields.

We select stars in a 5^{th} radius around the transient location (Figure 1). This translates to 50 pc at the distance of NGC 300 (2.0 M pc), which is a compromise between including as many coeval stars as possible while limiting contamination (see §4.3.4 for a discussion of the choice of selection radius). The CMD shows a truncated main sequence, indicating that star formation in this region terminated more than 5 Myr ago. However, the CMD shows no core helium burning stars, suggesting that there was no significant star formation during the interval between 25 and 300 Myr ago. Thus, even without a detailed analysis, the CMD alone indicates that the transient was due to a massive star that formed during a burst of star formation between 5 and 25 Myr ago. In the next section, we analyze the SFH in depth, giving tighter constraints on the age.

3. Analysis

3.1. Star Formation History

Overlaying isochrones on a CMD is the traditional method of determining the age of a young stellar population; however, this method relies on only a few main-sequence stars to establish age. In contrast, fitting the entire CMD uses the full wealth of information and can give tighter age constraints. Comparing the observed CMD to a set of model CMDs to derive the star formation history (SFH) is a well-established technique (Hernandez et al. 1999; Gallart et al. 1999; Holtzman et al. 1999; Dolphin 2002; Skillman et al. 2003; Harris & Zaritsky 2004; Gallart et al. 2005). While there are many different codes available, the basic procedure is the same for all: stellar evolution models are used to predict the properties of stars of different masses for a range of ages and metallicities. From the predicted luminosity and temperature, the magnitudes of the stars are determined for a given filter set. For each age and metallicity, stars are placed on a synthetic CMD in proportion to an assumed initial mass function (IMF). These CMDs are then linearly combined, with distance and extinction either fixed or included as additional free parameters, until the best fit to the observed CMD is found. The ages and metallicities of the CMDs that went into the best fit tell us the ages and metallicities of the underlying stellar population, while the weights given to the CMDs provide the SFR at each age.

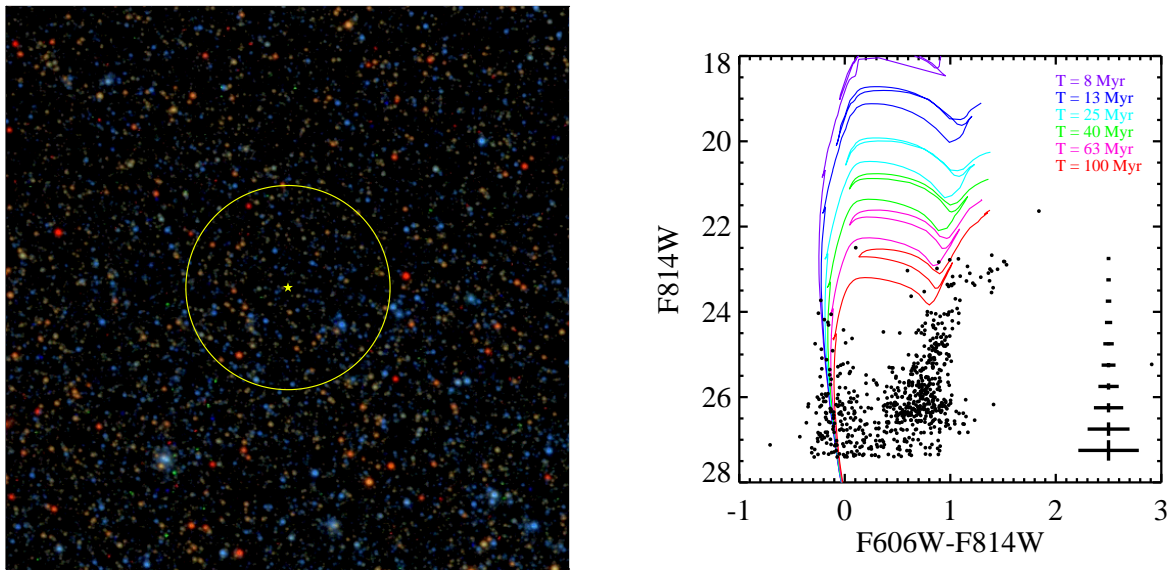


Fig. 1. | Left: subsection of the 3-color (F 475W ;F 606W ;F 814W) 2006 ACS in age of NGC 300. The location of the transient is marked with a star, while the circle indicates the 5° radius from which we selected stars. North is up and east is to the left. Right: CMD of stars in the selected region. Photometric errors as a function of F 814W magnitude are shown on the right. Isochrones corresponding to the edges of our age bins for SFH derivation are plotted. All isochrones are from Marigo et al. (2008) and have $[M/H] = 0.4$, $A_V = 0.1$, and $m - M = 26.5$.

To derive the SFH for NGC 300 OT2008-1, we use MATCH, which finds the maximum-likelihood fit to the CMD (Dolphin 2002). We assume an IMF with a slope of -2.35 (Salpeter 1955) and a binary fraction of 0.35. MATCH only allows a single value for the slope of the IMF, but given that our CMD only includes stars with masses $> 1 M_{\odot}$, adopting a single Salpeter slope is likely to be a valid assumption. Synthetic CMDs are constructed from the theoretical isochrones of Marigo et al. (2008) for ages in the range 4 Myr–14 Gyr. The isochrones younger than 6×10^7 yr were adopted from Bertelli et al. (1994), with transformations to the ACS system from Girardi et al. (2008). Age bins are spaced logarithmically since the CMD changes much more rapidly at young ages than at old ages. The edges of the age bins shown in this paper are 4 Myr (the age of the youngest isochrone), 8, 13, 25, 40, 63, and 100 Myr. Additional age bins go back to 14 Gyr.

Metallicity is constrained to increase with time within the range $-2.3 < [M/H] < 0.1$. As additional free parameters, the distance modulus is allowed to vary in the range $26.3 < m_M < 26.7$ and extinction can vary in the range $0.05 < A_V < 0.50$. Also, up to 0.5 mag of differential extinction may be applied to young stars (< 100 Myr). The Schlegel et al. (1998) value for Galactic extinction is $A_V = 0.042$ in the line of sight to NGC 300, but we expect the total value to be higher due to local extinction within NGC 300 itself.

Comparisons to model CMDs were carried out within bins of width 0.1 mag in color and 0.2 mag in magnitude. For a small number of stars, choosing bins that are too small results in so few stars in each bin that the accuracy of the fitting suffers. Our choice of bin size reduces this problem while ensuring that the number of bins in the CMD is substantially larger than the number of free parameters in the fit.

Completeness and photometric biases were accounted for by including the results of the artificial star tests. We supplied MATCH with the input and output magnitudes of the artificial stars and whether they were detected above the quality cuts of our photometry. We include only the portion of the F606W + F814W CMDs that were more than 50% complete, which corresponds to magnitudes of $F606W < 27.9$; $F814W < 27.0$ for the ANGST data and $F555W < 27.6$; $F814W < 27.0$ for the archival data. We also recovered the SFH using the F435W = F475W + F814W filter combinations and found consistent results, but since the depth in the B equivalent filters is less than in the V equivalent filters (F555W = F606W), the error bars on the resulting SFHs were considerably larger.

The resulting SFH of this region over the past 100 Myr is shown in Figure 2. The SFH shows a single star formation event in the range 8–13 Myr ago, with no significant additional star formation in the age range of 0–100 Myr. This isolated burst is the likely source of the progenitor. The time of the star formation event agreed between the ANGST-derived and archival-derived SFHs, with the amplitudes of the star formation events agreeing within the error bars. We note that many of the fainter stars in this region were formed at a low SFR over the past 14 Gyr; however, we plot only the past 100 Myr to highlight the event that likely produced the progenitor.

Error bars in Figure 2 are the quadrature sum of the errors from uncertainties in distance

and extinction and the 68% confidence interval from Monte Carlo tests, which assess uncertainties due to limited numbers of stars. Monte Carlo simulations were run by sampling stars from the best fitting model CMD determined by MATCH. These stars were then given as the input to MATCH, and the resulting SFH was compared to the SFH from which they were drawn. This process was repeated 100 times, and the scatter in difference between the input and output SFHs was incorporated into the error bars in our reported SFHs for each region. These trials indicated that the residual recent star formation at ages older than the burst was unlikely to be real, and that the SFH within the past 50 Myr could be explained entirely with a single burst. Monte Carlo simulations assess uncertainties due to Poisson sampling of underpopulated regions in the CMD, but they are not sensitive to systematic uncertainties in the models themselves. Hence, our error bars for the SFH do not include model uncertainties, but should be viewed as the range of possible values for this particular set of models. We discuss model uncertainties further in section 4.3.5.

Extinction was found to be $A_{F606W} = 0.09 \pm 0.04$. Gieren et al. (2005) find a total reddening for NGC 300 of $E(B - V) = 0.096 \pm 0.006$ mag, which corresponds to an extinction of $A_V = 0.3$ assuming the extinction law of Cardelli et al. (1989). Given that the extinction in NGC 300 varies with position (Roussel et al. 2005), it is not surprising that the value for this particular region is smaller. Berger et al. (2009) estimate the extinction of the transient itself from SED fitting (after much of the dust surrounding the progenitor may have been destroyed) and find $A_V = 0$ with a 1 σ upper limit of $A_V < 0.6$. Our value is consistent with this estimate also, although we note that the value we derive is the average extinction of the stars around the transient and not of the transient itself, which would include the circumstellar dust that prevented the detection of the progenitor at optical wavelengths. Bond et al. (2009) find from their spectroscopy that the transient itself could be reddened by as much as $E(B - V) \sim 0.4$, corresponding to an extinction of $A_V \sim 1.2$.

The best-fit distance modulus was found to be 26.41 ± 0.09 , which agrees with the value of 26.50 found using the tip of the red giant branch for the entire ACS field (Dalcanton et al. 2009), as well as previous distance estimates (Butler et al. 2004; Gieren et al. 2005; Rizzi et al. 2006); however, this is by construction given the limits placed on the distance modulus.

The current metallicity returned by MATCH is $[M/H] = -0.44 \pm 0.17$, which is in agreement with the value of $[M/H] = -0.27 \pm 0.15$ at this galactocentric radius (2.7 kpc) from the observed metallicity gradient of Kudritzki et al. (2008). To test the effect of metallicity on our results, we fixed the metallicity at $[M/H] = -0.7 \pm 0.1$ when deriving the SFH. The SFH still shows a burst at 8.13 Myr ago, though with an increased probability of the burst beginning earlier (20 Myr ago), presumably due to redder stars being interpreted as older rather than more metal-rich. Forcing the stars to be at solar metallicity results in a burst that is too young, 4.10 Myr ago, but that scenario is clearly inconsistent with the measured metallicity at this radius.

3.2. Mass of Progenitor

The relationship between stellar age and the main-sequence turn mass is plotted in Figure 2 (Marigo et al. 2008). From this plot we can infer the progenitor mass for a stellar population of a given age. The star formation event which gave rise to the transient happened between 8 and 13 Myr ago, which corresponds to a main sequence turn mass that falls in the mass range of $12\text{--}17 M_{\odot}$. Assuming that the transient was due to an evolving star, the transient precursor had a mass higher than this lower limit.

To determine the uncertainty in our turn mass estimates, we ran a series of Monte Carlo tests using artificial star formation bursts of varying amplitudes and durations and measured how well these SFHs could be recovered. We varied the amplitude of the bursts (i.e. SFR or number of stars formed in a constant time period), the start and end times of the burst (for varying duration), and the age of the burst for similar durations. Each simulation was repeated 50 times.

The amplitude trials were set so as to produce a certain number of upper main sequence stars (defined as $F_{606W} - F_{814W} < 0.3$ and $F_{606W} < 26$). Trials were run with numbers of approximately 25, 50, 100, and 150 (exact numbers varied slightly with each trial, since CMDs were created by sampling from the fixed SFH). The burst duration was set to 8–13 Myr to match the derived SFH of NGC 300 OT 2008-1. Results are shown in Figure 3. If each burst were perfectly recovered by MATCH, the cumulative distribution would go from 0 to 1 within the gray shaded region which shows the burst duration. All of the trials have a tail to older ages and smaller masses, indicating the tendency of MATCH to interpret stars as older than they really are, but this accounts for less than 40% of the total star formation in all cases with 50 or more upper main-sequence stars. The star burst with 50 upper main-sequence stars is the closest match to the derived SFH, which had 55 upper main-sequence stars. We see that the burst is not well constrained with only 25 upper main sequence stars, but it is at 50 and above. We conclude that at least 50 upper main-sequence stars are required to use this method.

We next set all duration trials to produce approximately 50 upper main-sequence stars, and then varied the starting and ending times of the burst. The end time trials began at 13 Myr ago and ended at 5, 6, and 10 Myr, and the start time trials began at 10, 16, and 20 Myr ago and ended at 8 Myr (Figure 4). These can be compared with the 8–13 Myr burst from Figure 3. We see that very short duration bursts (2–3 Myr) are not able to be recovered, with the resulting SFHs extending to significantly younger and older ages. Longer bursts are better constrained, especially at the upper turn mass limit. Despite the long tail to older ages, this actually represents a small range in absolute turn masses, as the 7–10 Myr range stretches over almost 20 Myr.

Since we used logarithmic time binning, we could not fix a constant linear time duration for a variety of ages, so instead we chose the time bins which gave durations as close as possible to the derived duration of 4.6 Myr. Figure 5 shows the results of these trials, with start times of 4, 5, 6, 10, 16, and 20 Myr ago. From these plots we conclude that bursts of this length are more easily recovered at more recent times. Bursts that ended more than 10 Myr ago are frequently interpreted

as ending more recently. We speculate that this problem may be related to poor sampling. If upper main-sequence stars are present, the CMD must be young, but the absence of these stars could be due to chance at the low levels of star formation that we are probing. Bursts with very recent end times show no tails to more recent ages because the youngest isochrones in our models are at 4 Myr.

We use a subset of these tests to assess the uncertainty in our mass estimate. The question we are asking is whether a burst that started earlier or ended later might be interpreted by MATCH as the 8{13 Myr burst we derived, and with what probability this might occur. For the start time variation, we define a "matching" burst as one that has a $SFR < 10^5 M_{\odot} \text{ yr}^{-1}$ for ages older than 13 Myr and a $SFR > 10^4 M_{\odot} \text{ yr}^{-1}$ at some point in the 8{13 Myr range. These cutoff values are taken from the derived SFH of NGC 300 OT2008-1, which has $SFR > 10^4 M_{\odot} \text{ yr}^{-1}$ during the burst and $< 10^5 M_{\odot} \text{ yr}^{-1}$ at other times. For the end time variation, we likewise define a "matching" burst as one that has a $SFR < 10^5 M_{\odot} \text{ yr}^{-1}$ for ages younger than 8 Myr and a $SFR > 10^4 M_{\odot} \text{ yr}^{-1}$ at some point in the 8{13 Myr range. We ran 50 additional Monte Carlo tests for these bursts, for a total of 100, but the results remained the same as for the original 50 runs testing the recovery of burst duration.

Of the bursts that started earlier (8{16 Myr and 8{20 Myr ago, top center and right panels in Figure 4), we found that the probabilities of recovering a single 8{13 Myr burst were 40% and 22%, respectively. This means that if we derive an 8{13 Myr burst for an observed CMD, we can be 60% sure that the burst started after 13 Myr ($M_{\text{prog}} > 12.4 M_{\odot}$) and 78% sure that it started after 16 Myr ($M_{\text{prog}} > 11.9 M_{\odot}$). Of the bursts that ended later (6{13 Myr and 5{13 Myr ago, bottom left and center panels in Figure 4), we found probabilities of 30% and 26%, respectively. Thus, we can be 70% certain that the burst ended by 8 Myr ago ($M_{\text{prog}} < 17 M_{\odot}$) and 74% certain that it ended by 6 Myr ago ($M_{\text{prog}} < 20 M_{\odot}$). Based on these tests, we report our uncertainty on the 12{17 M_{\odot} turnoff mass estimate as 70% (± 1 in a Gaussian distribution), setting the lower limit to the transient precursor mass.

At the higher mass end, the mass of the precursor is limited by the most massive post-main sequence star that is expected to exist for a burst of star formation between 8{13 Myr ago. As we show in Figure 6, isochrones for 8{13 Myr old bursts show no stars currently more massive than 16{25 M_{\odot} , with $\sim 1 M_{\odot}$ variation between different stellar models. If these models are correct, then the progenitor mass lies above 12{17 M_{\odot} but below 16{25 M_{\odot} .

To test the effect of varying the IMF and binary fraction on our results, we generated artificial SFHs with a burst from 8{13 Myr, distance modulus of $m - M = 26.5$, extinction of $A_{F606W} = 0.1$, and metallicity of $[M/H] = -0.4$, matching what we derived for the region surrounding NGC 300 OT2008-1. We varied the IMF from $\alpha = 2.0$ to $\alpha = 2.7$ for a binary fraction of 0.35, and varied the binary fraction from 0.2 to 0.5 with a Salpeter IMF of $\alpha = 2.35$. We ran MATCH on each of these models assuming a Salpeter IMF and binary fraction of 0.35, as in our original SFH derivation, to see if the age of the recovered burst changed with the input IMF or binary fraction.

We found that the only changes were in the amplitude of the burst, as expected since changing the IMF changes the normalization of the SFH, and that in each case MATCH still recovered a burst of $8\{13$ M yr. Hence, even if the IMF or binary fraction is different from our assumed value, it should not affect our age or mass estimates.

4. Discussion

4.1. Implications for SN 2008S/NGC 300 OT 2008-1-type Transients

Both NGC 300 OT 2008-1 and the similar transient SN 2008S have very highly obscured progenitors that are bright point sources at mid-infrared wavelengths but are undetectable in the optical. The spectrum of SN 2008S is similar to a SN II spectrum, but many scenarios, including the outburst of a star, are consistent with the low velocities implied by the narrow lines (Dessart et al. 2009). To date, two possible explanations have been put forward to explain this class of luminous transient. Thompson et al. (2008) suggest that the progenitors were heavily dust enshrouded AGB stars of mass $\sim 10 M_{\odot}$ with a photospheric radius in the mid-IR of a few hundred AU, and that the transients may have been electron-capture SNe. Botticella et al. (2009) also endorses the electron-capture SN explanation for these transients, with a mass estimate of $6\{8 M_{\odot}$ for SN 2008S. Alternatively, Smith et al. (2009) argue that the transient may be due to a super-Eddington wind being driven from a $\sim 20 M_{\odot}$ star. The SED and light curve of M 85 OT 2006-1 are also very similar to NGC 300 OT 2008-1 and SN 2008S (Kulkarni et al. 2007), with a mass estimate on the low end, $\sim 7 M_{\odot}$ (Oefek et al. 2008).

The $12\{17 M_{\odot}$ main-sequence turn mass we have derived as a lower limit for the precursor is in between the mass ranges suggested for both the electron-capture SN in an AGB star ($6\{11 M_{\odot}$, Thompson et al. 2008; Botticella et al. 2009) and the wind mechanism suggested by Smith et al. (2009). Although Smith et al. (2009) suggests a rough lower limit of ~ 15 solar masses for the super-Eddington wind, there are no theoretical arguments that would exclude lower masses. Given both the uncertainty in these mass ranges and the possibility that our data is consistent with a mass as high as $25 M_{\odot}$ or as low as $11 M_{\odot}$, we cannot at present rule out either option.

Our mass estimate is consistent with the $10\{15 M_{\odot}$ estimate of Bond et al. (2009) from Spitzer mid- to far-infrared fluxes. They infer an outflow from the spectrum of the transient, and propose an OH/IR star which erupted and cleared its surrounding dust envelope. Berger et al. (2009) find evidence of infall as well as outflow in their high-resolution spectra. Using a similar interpretation to Smith et al. (2009), they suggest a blue supergiant or Wolf-Rayet star and give a more generous mass estimate of $10\{20 M_{\odot}$, also fully consistent with our derived SFH.

4.2. The Red Supergiant Problem

The progenitor mass for NGC 300 OT 2008-1 reported in this paper has interesting implications for stellar evolution theory. Prior to SN 2008S and NGC 300 OT 2008-1, episodic mass loss evident in LBV outbursts and SN II_n was associated only with the most massive ($> 20 M_{\odot}$) stars (Smith et al. 2004; Gal-Yam et al. 2007; Smith 2007). Whether NGC 300 OT 2008-1 is an electron-capture SN (Prieto et al. 2008a; Thompson et al. 2008) or a non-disruptive outburst analogous to LBV eruptions (Smith et al. 2009; Berger et al. 2009), the narrow emission lines are a signature of significant mass loss at speeds lower than a typical SN. In either case, the association of a progenitor mass as low as $15 M_{\odot}$ with an outburst and implied episode of mass loss is a new and somewhat unexpected result. Perhaps the only obvious analog is SN 1987A, which was a $20 M_{\odot}$ blue supergiant just before explosion (Woolsey et al. 1987; Walborn et al. 1987; Woolsey et al. 1988; Woolsey 1988; Amett 1991). Its progenitor was likely a red supergiant (RSG) $\sim 30,000$ yr earlier (Fransson et al. 1989), and may have made the transition via a LBV-like eruption (Smith 2007). Might NGC 300 OT 2008-1 be the signature of a similar transition?

Whether significant mass-loss events are common for stars $< 20 M_{\odot}$ has important consequences for our understanding of stellar evolution, especially during the last stages. If the cumulative effect of events like NGC 300 OT 2008-1 is to expel a significant fraction of the hydrogen envelope, then we know that not all $8\{20 M_{\odot}$ stars experience such events, since the most common type of SN, SN II-P, originate from stars in this mass range. However, Smartt et al. (2009) have identified a potential lack of SN II-P progenitors more massive than $16.5 \pm 1.5 M_{\odot}$. RSGs, the progenitors of SN II-P, should be common up to a maximum mass of at least $25 M_{\odot}$, since more massive stars will become Wolf-Rayet stars (e.g., Crowther 2007). Although statistically some SN progenitors of masses $17\{25 M_{\odot}$ should have been in the volume-limited sample of Smartt et al. (2009), they report with 2:4 confidence that RSGs in this mass range are not exploding as SN II-P as expected. Smartt et al. (2009) consider several resolutions to this problem, including the idea that stars in this mass range explode as another type of SN, but they favor the idea that the minimum progenitor mass for black hole formation is lower than expected, resulting in failed or weak SN II for this mass range.

Intriguingly, the progenitor mass we find for NGC 300 OT 2008-1 is consistent with the mass range that defines the onset of the SN II-P decay, and the event itself could signify the transition away from a RSG phase. We consider whether stars in the mass range $17\{25 M_{\odot}$ experience optical transients (OTs) and episodic mass-loss, expelling much or some of their hydrogen envelopes and aborting a connection to SN II-P. Using the observed rate of SN II-P and assuming the Salpeter IMF, we can estimate the minimum number of NGC 300 OT 2008-1-like transients necessary to explain the RSG problem. If we assume that a minimum of one OT per star is necessary to keep it from exploding as a SN II-P, integrate the IMF from 17 to $25 M_{\odot}$, and compare this to the IMF integrated from 8 to $17 M_{\odot}$, this gives us a minimum OT-to-SN II-P ratio of 0.23 to explain the lack of high mass SN II-Ps.

Smartt et al. (2009) report 54 SN II-P in their volume limited (< 28 Mpc) survey during a span of 10.5 years. The deficit of higher mass SN II-P progenitors suggests that (in steady state) at least 12 additional stars within the same volume must have shed some of their hydrogen envelopes in an OT during the duration of the survey; an even higher rate of OTs may be expected if multiple mass loss events are needed to fully strip the hydrogen envelope. Three similar transients were reported between 2006 and 2008, one in 2006 and two in 2008 (Berger et al. 2009). They are NGC 300 OT 2008-1 at 2 Mpc, SN 2008S at 4 Mpc, and M 85 OT 2006-1 at 17 Mpc. If we take this as a rough rate of OTs, then the number of OTs over the > 10 yr span of the Smartt et al. (2009) survey is 11, and within a smaller survey volume. Therefore, the observed rate of OTs is not inconsistent with this type of event being sufficient to explain the paucity of high mass SN II-P progenitors between 17 and 25 Mpc. However, given the uncertainties and small sample size in the Smartt et al. (2009) mass estimates, the different effective survey volumes for SN II-Ps and OTs, and the lack of a secure progenitor mass for SN 2008S, we cannot yet draw a firm conclusion.

4.3. Limitations of the Method

The work above demonstrates that one can obtain accurate precursor masses even when the actual precursor is undetected. Although the images we used were taken several years before the transient, there was nothing in the analysis that required direct identification of the precursor. Instead, the mass was derived through "guilt by association" using the properties of the underlying burst of star formation. In principle, one could use this method to derive masses of precursors of every transient or SN in the historical record. In practice, however, this method is somewhat more limited.

4.3.1. Crowding

Recovery of recent SFHs requires CMDs of individual main-sequence and helium-burning stars. However, images of individual stars are blurred together, with the crowding being more severe at larger distances, in high surface brightness regions, and/or for fainter stars (which are more numerous). Even with HST's resolution, crowding quickly limits the ability to measure fluxes for all but the brightest stars beyond 45 Mpc. The crowding limit can be reached in any magnitudes brighter than one would expect for a given telescope aperture and exposure time. This limitation is less of a problem for stars on the blue and red helium-burning sequences, which are far more luminous than main-sequence stars of comparable masses. However, these sequences are only well-populated after 25 Myr, making them useful only for low mass precursors ($M < 9 M_{\odot}$). Thus, crowding is a significant limitation on the applicability of this method, at least until the launch of telescopes that can surpass HST's angular resolution in the optical. Advances in infrared space telescopes may not bring much progress, given the faintness of main-sequence stars in the infrared.

4.3.2. Depth

Even when crowding is not significant for a main sequence star of a given stellar mass, the SFH method requires depths that are a magnitude or more below the main-sequence turn of the stellar masses of interest. The recent star formation is largely constrained by the luminosity function of the main sequence, so that the behavior on the more sparsely populated upper main sequence is forced to be consistent with the numbers of stars on the lower main sequence. Thus, bursts are best constrained when the main sequence is well-measured substantially below the turn.

4.3.3. Very Massive Stars

While the modeling in this paper yielded excellent limits on the mass of this particular precursor, we anticipate larger uncertainties for higher mass precursors, for several reasons. First, the optical luminosity of a very massive main-sequence star is a tiny fraction of its bolometric luminosity, making optical CMDs poor constraints on the masses of the most massive stars. The masses of the most massive main sequence stars can only be accurately determined through spectroscopy (Massey 2003), given that stars with $T > 30,000\text{K}$ have essentially identical optical and near-UV colors. Thus, while using SFHs to measure precursor masses may work for up to $20\{30 M_{\odot}$, it is less likely to be useful for higher masses.

Second, the very youngest, most massive stars are likely to remain shrouded within their natal molecular clouds to some extent. If these stars have not emerged from their dust cocoons by $\sim 5\text{ Myr}$ (the turn age of a $25 M_{\odot}$ star), then their measured luminosities and colors are likely to be significantly affected by dust, causing the main sequence to broaden to the red and to shift to lower luminosities. SFH recovery codes typically take dust into account statistically by including a "differential reddening" term to help match the width and position of the main sequence. However, this correction cannot compensate for stars that are simply absent due to very high dust extinction; observations in the Magellanic clouds suggest that this effect is significant for ages less than 2 Gyr (Massey et al. 1995). Dust can also be corrected for on a star-by-star basis, provided that imaging on the UV side of the Balmer break is included (Romaniello et al. 2002).

Third, very massive stars are likely to be found within dense stellar clusters that have not yet experienced significant cluster dissolution. The timescale for this dissolution is $\sim 10\text{ Myr}$, such that 50% of stars with mass $15 M_{\odot}$ are likely to still be bound into clusters (Lada & Lada 2003; Bastian et al. 2005). These clusters have higher than average crowding, and thus stars within them are prone to larger photometric errors and brighter limiting magnitudes.

Finally, the upper main sequence is always less populated than the lower, making it statistically possible that the youngest apparent "turn" in the main sequence appears to be older than the true turn, due to the sparse sampling of the high mass end of the IMF.

4.3.4. Region Size

An additional concern with the method is the choice of region size. If the radius within which stars are selected is too small, it is possible that stars will have dispersed from an unbound cluster to beyond this radius. However, the dispersal timescale is tens of Myr, as the stars are expected to disperse with the typical cluster velocity dispersion of a few km s^{-1} (Bastian & Goodwin 2006). In the 5^{th} (50 pc) region we selected, if the cluster velocity dispersion is $1 \text{ km s}^{-1} = 1 \text{ pc Myr}^{-1}$ (a reasonable value for a small cluster), stars would still be contained within the region after 50 Myr, which is longer than the estimated timescale of star formation for this cluster. For a larger cluster with a velocity dispersion of 3 pc Myr^{-1} , the stars would remain within 50 pc for 17 Myr, still longer ago than the beginning of the star formation event we see in this region.

Choosing a larger radius would ensure that all stars from the cluster are included; however, a larger radius also increases contamination from surrounding unrelated stars. We find that using a radius of 7.5^{th} instead of 5 (2.25 times the area enclosed) results in a less well-defined burst, probably because we are enclosing stars slightly older than the population which gave rise to the transient.

4.3.5. Choice of Stellar Evolution Models

We have used the isochrones from the Padova group (Marigo et al. 2008) in our analysis, and the errors reported assume that those models are correct. However, additional systematic errors may be introduced by uncertainties in the models. Gallart et al. (2005) provide an in-depth discussion of the discrepancies between different models and their effect on deriving SFHs using CMD fitting, and they conclude that the uncertainties seem to be smallest for young stars, which is reassuring for studies of transient progenitors. To assess the errors in more detail, we compare the Padova models with the currently available Geneva models (Lejeune & Schaerer 2001). Both sets of models include the effects of convective core overshooting, but not rotation. The Padova models include thermal pulses on the AGB, while the Geneva models do not.

Figure 6 shows isochrones from the two models for ages 8 Myr and 13 Myr, the ranking ages of the star formation event we found for NGC 300 OT 2008-1. Metallicity is $Z = 0.008$ ($[M/H] = -0.4$). The left panel plots the isochrones for both models for each age, with the main-sequence turn magnitude marked. The models are very similar up to the turn, and diverge for more massive stars. We are especially concerned with the mapping between age and stellar mass, since we use this relationship to go from an age estimate to a stellar mass estimate for the NGC 300 OT 2008-1 progenitor, so we plot mass as a function of absolute magnitude for the same isochrones in the right panel of Figure 6. For each age, the mass-luminosity relationship is identical between the models up until the main-sequence turn, but there are discrepancies above the turn. Since the age of a young stellar population is primarily determined by the main sequence, we expect that differences in the models related to the treatment of post-main-sequence phases will not significantly affect

our results.

A potentially significant effect not addressed in the previous comparison is rotation. For solar metallicity and an initial rotation velocity of 200 km s^{-1} , the age estimate for a star of a given luminosity would increase by about 25% from the non-rotating model (Meynet & Maeder 2000). Hence, including rotation in the models would increase our age estimate for the star formation event to $10\{16 \text{ Myr}$ and the upper mass limit for the tumo would decrease to $15 M_{\odot}$. The lower mass limit for the tumo changes from $12.3 M_{\odot}$ to $11.9 M_{\odot}$. Hence, even including the effects of rotation at this velocity, our tumo mass range of $12\{17 M_{\odot}$ is still valid. Rotation speeds in excess of 200 km s^{-1} could lead to smaller possible masses for the progenitor. Vazquez et al. (2007) show that the decrease in main sequence lifetime also holds for stars at $Z = 0.008$ (the approximate metallicity of the region around the transient), but isochrones for this metallicity are only available for masses $> 30 M_{\odot}$.

4.3.6. Ambiguous Bursts

The natural possible limitation is that Nature may not always be as kind as she has been in this particular instance. While NGC 300 OT2008-1 came from an unambiguous isolated burst, some transient phenomena may be associated with regions containing multiple bursts at a range of ages, making the association of mass ambiguous. This effect is more likely to be pronounced in more distant galaxies, where a typical aperture size of a few arcseconds encompasses a larger physical area of the disk, and thus is more likely to contain more than one dissolving open cluster. On the other hand, the analysis of star formation regions in M 81 (D = 3.7 Mpc) presented in Gogarten et al. (2009) uses $\sim 2700 \times 500 \text{ pc}$ regions, and finds bursts that are well localized in time up to 100 Myr .

4.4. Benefits of the Method

In spite of the above limitations, there are a number of clear benefits to the procedure we have demonstrated in this paper. The first and most obvious one is the removal of the need for precursor imaging in determining the mass. Instead, targeted observations after the event are sufficient, and can be optimized for recovery of the SFH, through proper choices of filters and observing strategy. Second, unlike in precursor imaging, one does not need accurate astrometry. Since the SFH recovery uses stars within a few arcsecond wide aperture, it is not required that the SN or transient be localized to better than half the width of the selection aperture. Third, given the uncertainties in the late stages of stellar evolution, it is perhaps easier to derive an accurate mass from the bulk properties of the better-understood main- and helium-burning sequences, rather than from the luminosity and SED of a star on the brink of explosion. Finally, the relationship between progenitor mass and SN type as predicted by stellar evolution models relies on assumptions about

mass loss during late stage stellar evolution. Contributions to the existing catalog of precursor masses using the SFH technique will improve the statistics in comparing observations with stellar evolution theory, and may even give more reliable initial mass estimates than can be determined from an individual star.

5. Conclusions

In this paper we have demonstrated a technique for measuring the masses of precursors of luminous transient events, even when no pre-event imaging exists. By using standard tools to recover the SFH from stellar populations, we find that NGC 300 OT 2008-1 originated from stars formed in a burst between 8 and 13 Myr ago with a certainty of 70%. The current turnoff mass associated with this burst is $12.17 M_{\odot}$. Assuming the transient is due to an evolving massive star, then the mass of the precursor must be higher than this turnoff mass, but less than the $16.25 M_{\odot}$ mass limit above which stars of this age have exploded. The resulting mass range of $12.25 M_{\odot}$ agrees quite well with estimates of $10.15 M_{\odot}$ by Bond et al. (2009) and $10.20 M_{\odot}$ by Berger et al. (2009). This technique therefore shows great promise for significantly expanding the number of SNe and transients with reliable precursor masses.

The SFH method presented here for determining precursor masses is largely complementary to direct precursor imaging, as each method has benefits and limitations. At present, the limits of the SFH technique are largely observational. The angular resolution of HST currently restricts this technique to well within $D < 10$ Mpc. In a future paper (Gilbert et al. 2009, in preparation), we will present an application of the method to all SNe and transients for which sufficiently deep data exists in the HST archive.

With future space-based optical telescopes one can certainly push the technique to much larger distances, greatly expanding the volume of candidate SNe. The more intensive monitoring of nearby galaxies can also significantly increase the number of SNe for which this technique can be used; thankfully such monitoring is currently underway (e.g., Leaman 2008; DiCarlo et al. 2008). The main benefits of the method are that imaging can be done after a transient event, even without accurate astrometry, and that fitting the entire main sequence of a star formation event may provide more reliable mass estimates.

In closing, we note that precursor imaging is still highly desirable. The technique we have employed gives only a constraint on the main-sequence mass of the star that eventually erupted. However, it gives no constraint on the exact phase of stellar evolution that the star was in immediately before the eruption. Precursor imaging can yield much more information about a star than its mass alone (e.g., color, magnitude). Given the impact of the unexpected phase of the SN 1987A precursor (i.e., that it was a blue, rather than red, supergiant at the time of explosion) on our understanding of core-collapse SNe, any additional information on the precursor is likely to be highly significant.

We thank Adam Burrows, Luc Dessart, Christian Ott, and Nathan Smith for helpful discussions. Leo Girardi provided the stellar evolution models used in this paper as well as a discussion of their uncertainties. We also thank the anonymous referee for comments which significantly improved the paper. Support for this work was provided by NASA through grant GO-10915 from the Space Telescopes Science Institute, which is operated by the Association of Universities for Research in Astronomy, Inc., under NASA contract NAS5-26555. S.M.G. was partially supported by NSF grant CAREER AST 02-38683. J.J.D. was partially supported as a Wycko Faculty Fellow. In addition, J.W.M. is supported by an NSF Astronomy and Astrophysics Postdoctoral Fellowship under award AST-0802315.

Facilities: HST (ACS)

REFERENCES

- Anderson, J. P., & James, P. A. 2008, *MNRAS*, 390, 1527
- Amett, D. 1991, *ApJ*, 383, 295
- Bastian, N., Gieles, M., Lamers, H. J. G. L. M., Scheepmaker, R. A., & de Grijs, R. 2005, *A & A*, 431, 905
- Bastian, N., & Goodwin, S. P. 2006, *MNRAS*, 369, L9
- Berger, E., & Soderberg, A. 2008a, *The Astronomer's Telegram*, 1543
- | . 2008b, *The Astronomer's Telegram*, 1544
- Berger, E. et al. 2009, *ApJ*, 699, 1850
- Bertelli, G., Bressan, A., Chiosi, C., Fagotto, F., & Nasi, E. 1994, *A & A S*, 106, 275
- Bond, H. E., Bedin, L. R., Bonanos, A. Z., Humphreys, R. M., Monard, L. A. G. B., Prieto, J. L., & Walter, F. M. 2009, *ApJ*, 695, L154
- Bond, H. E., Walter, F. M., & Velasquez, J. 2008, *IAU Circ.*, 8946, 2
- Botticella, M. T. et al. 2009, *MNRAS*, in press (arXiv:0903.1286)
- Butler, D. J., Martinez-Delgado, D., & Brandner, W. 2004, *AJ*, 127, 1472
- Cardelli, J. A., Clayton, G. C., & Mathis, J. S. 1989, *ApJ*, 345, 245
- Crockett, R. M. et al. 2008, *ApJ*, 672, L99
- Crowther, P. A. 2007, *ARA & A*, 45, 177
- Dalcanton, J. J., et al. 2009, *ApJS*, in press

- Dessart, L., Hillier, D. J., Gezari, S., Basa, S., & Matheson, T. 2009, *MNRAS*, 394, 21
- DiCarlo, E. et al. 2008, *ApJ*, 684, 471
- Dolphin, A. E. 2000, *PASP*, 112, 1383
- | . 2002, *MNRAS*, 332, 91
- Efronov, Y. N. 1991, *Soviet Astronomy Letters*, 17, 173
- Fransson, C., Cassatella, A., Gilmozzi, R., Kirshner, R. P., Panagia, N., Sonneborn, G., & Wamsteker, W. 1989, *ApJ*, 336, 429
- GalYam, A. et al. 2007, *ApJ*, 656, 372
- Gallart, C., Freedman, W. L., Aparicio, A., Bertelli, G., & Chiosi, C. 1999, *AJ*, 118, 2245
- Gallart, C., Zoccali, M., & Aparicio, A. 2005, *ARA&A*, 43, 387
- Gieren, W., Pietrzynski, G., Soszynski, I., Bresolin, F., Kudritzki, R. P., Minniti, D., & Storm, J. 2005, *ApJ*, 628, 695
- Girardi, L. et al. 2008, *PASP*, 120, 583
- Gogarten, S. M. et al. 2009, *ApJ*, 691, 115
- Harris, J., & Zaritsky, D. 2004, *AJ*, 127, 1531
- Heger, A., Fryer, C. L., Woosley, S. E., Langer, N., & Hartmann, D. H. 2003, *ApJ*, 591, 288
- Hernandez, X., Valls-Gabaud, D., & Gilmore, G. 1999, *MNRAS*, 304, 705
- Holtzman, J. A. et al. 1999, *AJ*, 118, 2262
- James, P. A., & Anderson, J. P. 2006, *A&A*, 453, 57
- Kelly, P. L., Kirshner, R. P., & Pahre, M. 2008, *ApJ*, 687, 1201
- Kudritzki, R. P., Urbaneja, M. A., Bresolin, F., Przybilla, N., Gieren, W., & Pietrzynski, G. 2008, *ApJ*, 681, 269
- Kulkarni, S. R. et al. 2007, *Nature*, 447, 458
- Lada, C. J., & Lada, E. A. 2003, *ARA&A*, 41, 57
- Leaman, J. F. 2008, PhD thesis, University of California, Berkeley
- Lejeune, T., & Schaerer, D. 2001, *A&A*, 366, 538

- Limongi, M., & Chieffi, A. 2007, in American Institute of Physics Conference Series, Vol. 924, The Multicolored Landscape of Compact Objects and Their Explosive Origins, ed. T. di Salvo, G. L. Israel, L. Piersanti, L. Burderi, G. Matt, A. Tomambè, & M. T. Menna, 226{233
- Maza-Apellaniz, J., Bond, H. E., Siegel, M. H., Lipkin, Y., Maoz, D., Ofek, E. O., & Poznanski, D. 2004, *ApJ*, 615, L113
- Marigo, P., Girardi, L., Bressan, A., Groenewegen, M. A. T., Silva, L., & Granato, G. L. 2008, *A & A*, 482, 883
- Massey, P. 2003, *ARA & A*, 41, 15
- Massey, P., Lang, C. C., Degioia-Eastwood, K., & Garmany, C. D. 1995, *ApJ*, 438, 188
- Meynet, G., & Maeder, A. 2000, *A & A*, 361, 101
- Monard, L. A. G. 2008, *IAU Circ.*, 8946, 1
- Ofek, E. O. et al. 2008, *ApJ*, 674, 447
- Panagia, N., Romaniello, M., Scuderi, S., & Kirshner, R. P. 2000, *ApJ*, 539, 197
- Prieto, J. L. 2008, *The Astronomer's Telegram*, 1550, 1
- Prieto, J. L. et al. 2008a, *ApJ*, 681, L9
- Prieto, J. L., Stanek, K. Z., & Beacom, J. F. 2008b, *ApJ*, 673, 999
- Rizzi, L., Bresolin, F., Kudritzki, R. P., Gieren, W., & Pietrzynski, G. 2006, *ApJ*, 638, 766
- Romaniello, M., Panagia, N., Scuderi, S., & Kirshner, R. P. 2002, *AJ*, 123, 915
- Roussel, H., Gilde-Paz, A., Seibert, M., Helou, G., Madore, B. F., & Martin, C. 2005, *ApJ*, 632, 227
- Salpeter, E. E. 1955, *ApJ*, 121, 161
- Schlegel, D. J., Finkbeiner, D. P., & Davis, M. 1998, *ApJ*, 500, 525
- Skillman, E. D., Tolstoy, E., Cole, A. A., Dolphin, A. E., Saha, A., Gallagher, J. S., Dohm-Palmer, R. C., & Mateo, M. 2003, *ApJ*, 596, 253
- Smartt, S. J., Eldridge, J. J., Crockett, R. M., & Maund, J. R. 2009, *MNRAS*, 395, 1409
- Smith, N. 2007, *AJ*, 133, 1034
- Smith, N. et al. 2009, *ApJ*, 697, L49
- Smith, N., Vink, J. S., & de Koter, A. 2004, *ApJ*, 615, 475

- Stanishev, V., Pastorello, A., & Pursimo, T. 2008, *Central Bureau Electronic Telegrams*, 1235, 1
- Thompson, T. A., Prieto, J. L., Stanek, K. Z., Kistler, M. D., Beacom, J. F., & Kochanek, C. S. 2008, *ArXiv e-prints*
- Van Dyk, S. D. 2007, *Highlights of Astronomy*, 14, 205
- Van Dyk, S. D., Peng, C. Y., Barth, A. J., & Filippenko, A. V. 1999, *AJ*, 118, 2331
- Vazquez, G. A., Leitherer, C., Schaerer, D., Meynet, G., & Maeder, A. 2007, *ApJ*, 663, 995
- Vinko, J. et al. 2009, *ApJ*, 695, 619
- Walton, N. R., Lasker, B. M., Laidler, V. G., & Chu, Y.-H. 1987, *ApJ*, 321, L41
- Walton, N. R., Phillips, M. M., Walker, A. R., & Elias, J. H. 1993, *PASP*, 105, 1240
- Wang, X., Yang, Y., Zhang, T., Ma, J., Zhou, X., Li, W., Lou, Y.-Q., & Li, Z. 2005, *ApJ*, 626, L89
- Williams, B. F. et al. 2009, *AJ*, 137, 419
- Woolsey, S. E. 1988, *ApJ*, 330, 218
- Woolsey, S. E., Heger, A., & Weaver, T. A. 2002, *Reviews of Modern Physics*, 74, 1015
- Woolsey, S. E., Pinto, P. A., & Ensmann, L. 1988, *ApJ*, 324, 466
- Woolsey, S. E., Pinto, P. A., Martin, P. G., & Weaver, T. A. 1987, *ApJ*, 318, 664

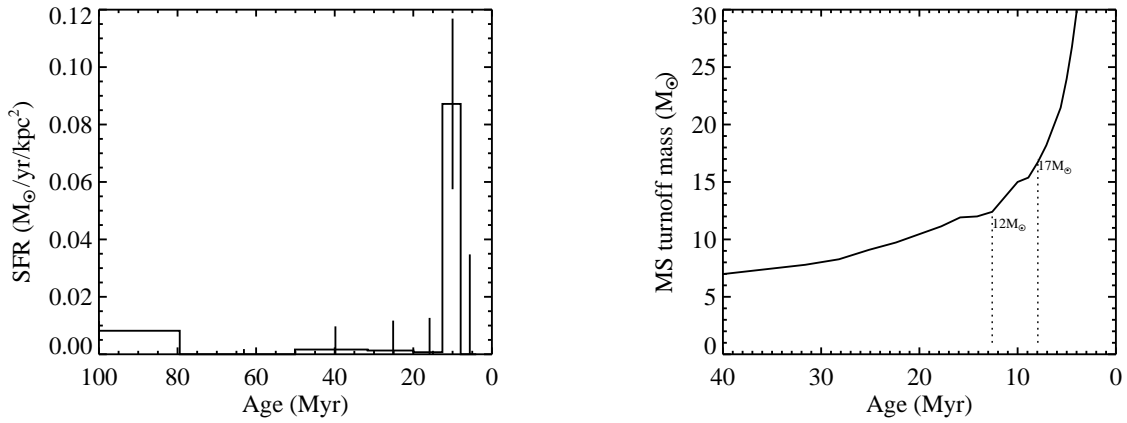


Fig. 2. | Left: recent star formation history (< 100 Myr) of the selected region in NGC 300, showing a significant star formation event at 8–13 Myr. SFH was found by comparing the observed ANGST CMD with synthetic CMDs based on theoretical isochrones. Error bars are the quadrature sum of the uncertainties from distance and extinction and the 68% confidence interval from Monte Carlo simulations. Right: main-sequence turnoff mass vs. age (Marigo et al. 2008). The boundaries of the star formation event and corresponding stellar masses are marked. These masses represent the lower limits on the mass of the transient.

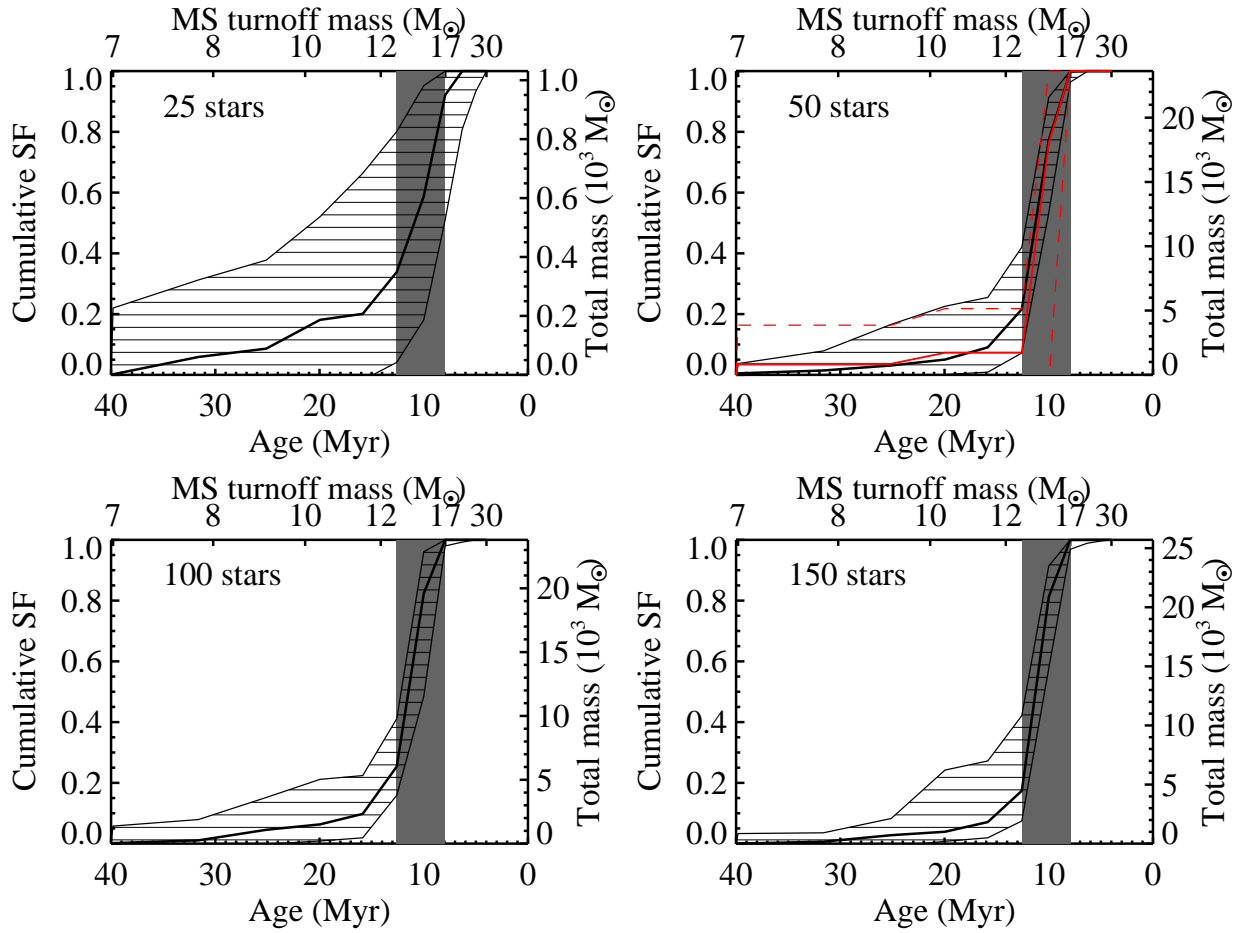


Fig. 3. Simulated bursts of age 8–13 Myr and varying amplitudes (gray shaded regions) and derived SFHs. The cumulative distribution functions show the total star formation summed from older ages to younger ages. The central black line is the median value of the Monte Carlo tests, and the surrounding hashed region is the 1- σ error range. Derived SFH and errors for NGC 300 OT 2008-1 are in red. The number of stars refers to upper main-sequence stars ($F 606W - F 814W < 0.3$, $F 606W < 26$).

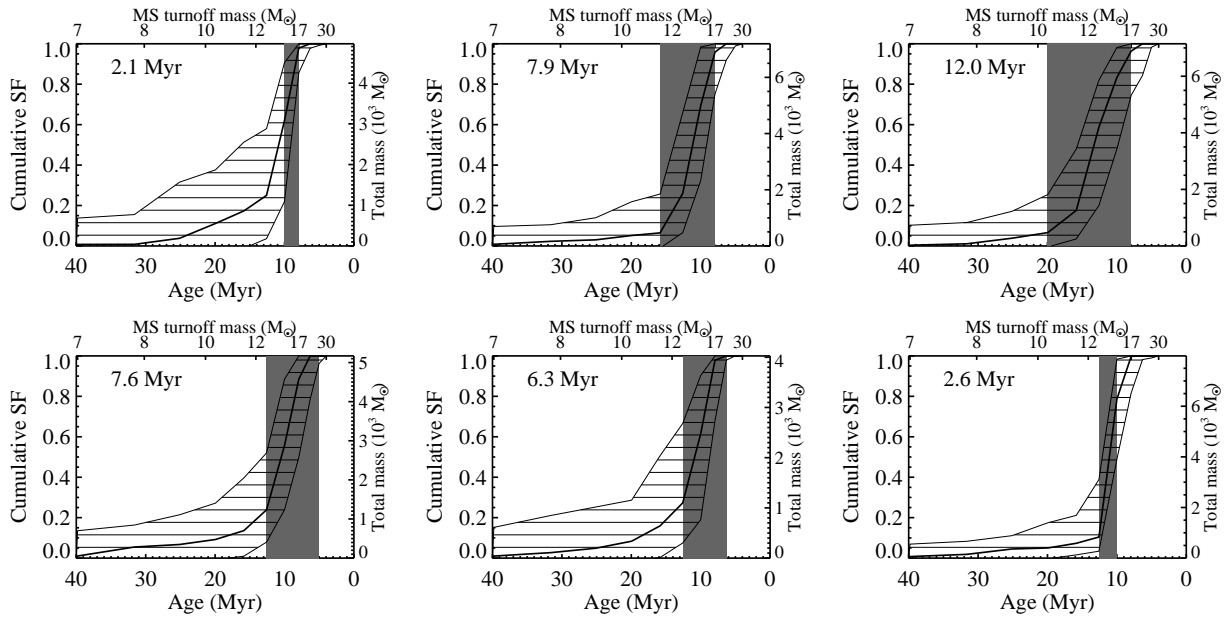


Fig. 4. | Simulated bursts with 50 upper main-sequence stars and varying durations (gray shaded regions) and derived SFHs. The central black line is the median value of the Monte Carlo tests, and the surrounding hashed region is the 1- σ error range. Upper row: constant end time (bursts start at 10, 16, and 20 Myr ago and end at 8 Myr); lower row: constant start time (bursts start at 13 Myr ago and end at 5, 6, and 10 Myr). Burst duration is labeled on each plot.

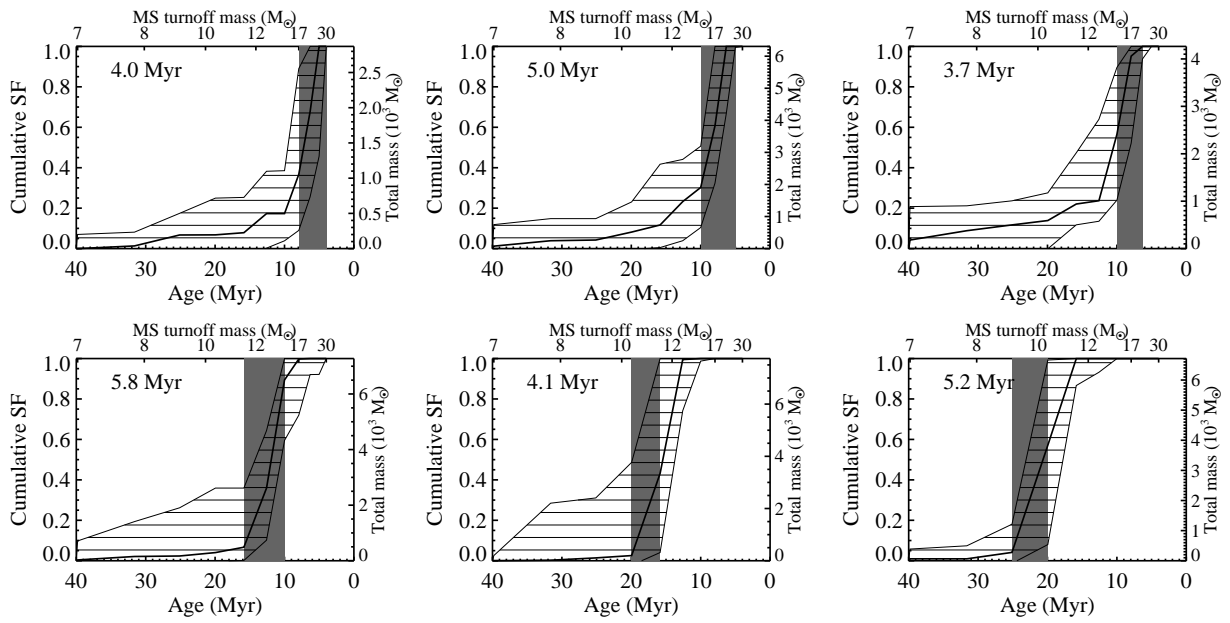


Fig. 5. | Simulated bursts with 50 upper main-sequence stars and varying ages (gray shaded regions) and derived SFHs. The central black line is the median value of the Monte Carlo tests, and the surrounding hashed region is the 1 σ error range. Upper row : burst ages are 4{8, 5{10, 6{10 M yr. Lower row : burst ages are 10{16, 16{20, and 20{25 M yr. Burst duration is labeled on each plot.

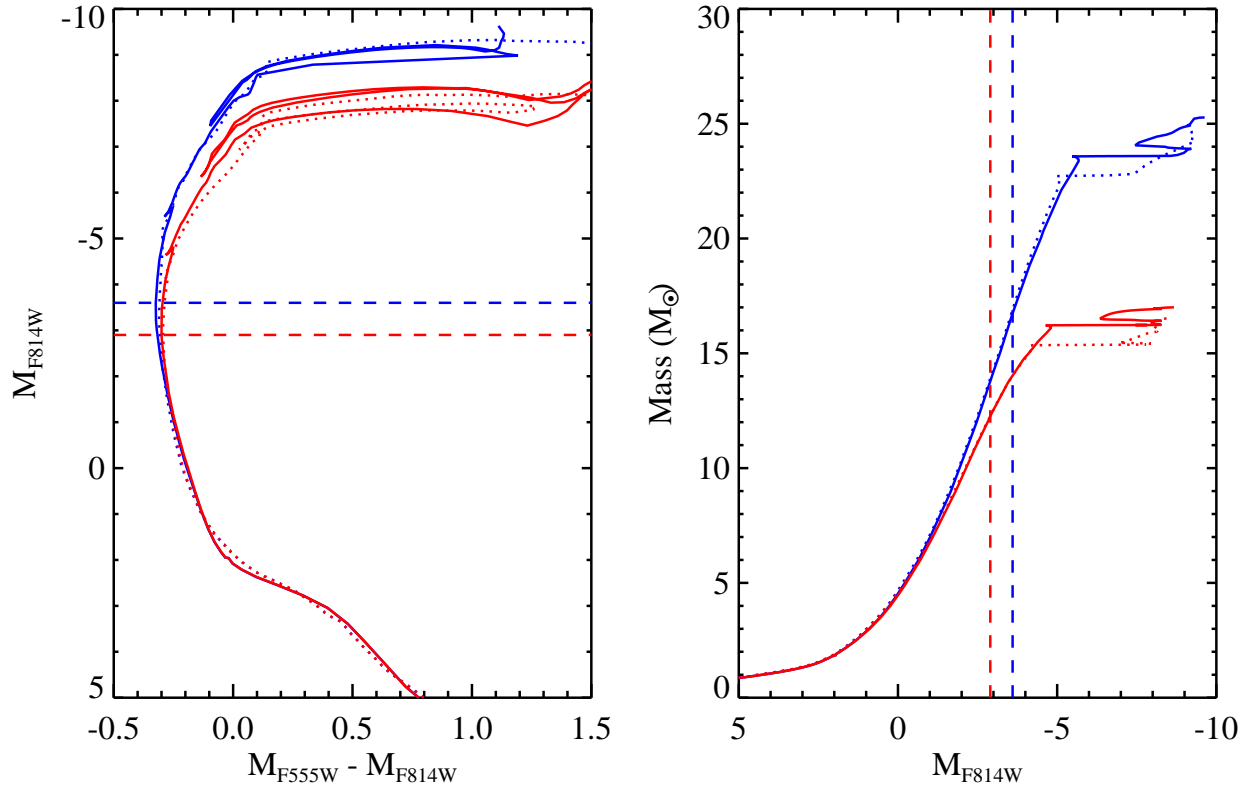


Fig. 6. Comparison of the Padova (Marigo et al. 2008, solid lines) and Geneva (Lejeune & Schaerer 2001, dotted lines) isochrones for $Z = 0.008$ and ages of 8 Myr (blue) and 13 Myr (red). The left panel shows the isochrones on a CMD, while the right panel shows stellar mass as a function of absolute magnitude. The magnitude of the main-sequence turn-off is highlighted with a dashed line for each age. The maximum masses shown by the endpoints of the isochrones cover a range of $16\text{--}25 M_{\odot}$. The two different isochrone sets agree well for main sequence stars, but show significant differences in their post-main-sequence evolution.